

# Electroless Nickel / Electroless Palladium / Immersion Gold Process For Multi-Purpose Assembly Technology

Kuldip Johal and Hugh Roberts, Atotech USA Inc.  
Sven Lamprecht, Atotech Deutschland GmbH

## ABSTRACT

As the second part to a paper presented at the 2004 SMTA Pan Pacific Symposium, this paper further summarizes the results from technical qualification of the Ni/Pd/Au process. Whereas the previous paper examined the wire bonding capabilities of this surface finish, this second paper focuses specific attention to BGA applications. In these investigations, the solder joint integrity is measured using ball shear testing of BGAs as test vehicles. Ball shear performance of BGA solder joints is examined using both eutectic solder and a tin-silver-copper (SAC) alloy. Testing of eutectic Sn-Pb solder joints demonstrates the impact of thermo-cycling (500 cycles of -55°C to +125°C) on the Ni/Pd/Au surface in comparison to other selective finish methodologies (i.e. electroless nickel/gold and organic solderability preservatives). Similarly, ball shear testing of the SAC-alloy solder joints shows the impact of thermal aging (+150°C for 1000 hours) on the Ni/Pd/Au surface, compared to the performance of the more conventional electrolytic nickel/electrolytic gold process under the same test conditions. The overall reliability of solder ball attachment is characterized by both mechanical ball shear test results and visual inspection.

Key words: Nickel, Palladium, Gold, BGA, SAC-alloy

## BACKGROUND

The use of micro ball grid arrays ( $\mu$ BGA), chip-scale packaging (CSP) and flip chip technologies for high-volume assembly of semiconductors has increased dramatically in the past several years. To keep pace with the rising level of semiconductor packaging sophistication, the printed circuit board fabrication and assembly technologies must also advance accordingly. To satisfy the current and near-future technology demands, the most significant challenge is usually finding a suitable coplanar bonding surface that offers reliable solderability, as well as dependable wire bonding (gold and aluminum) and consistent conductive adhesive printing dimensions. Furthermore, any method chosen must clearly be capable of working within the continuously decreasing circuitry geometry, as well as the upcoming lead-free requirements within the industry. According to conventional know-how, the electrolytic nickel/electrolytic gold process has normally been accepted as the

selective finish to meet the combined requirements of solderability and wire bondability. Electroless nickel/electroless gold is also used for such applications. Both of these processes are relatively costly due to the content of precious metal. Furthermore, neither process can be used for aluminum wire bonding. As a "universal" final finish, the electroless nickel / electroless palladium / immersion gold plating process (Ni/Pd/Au) offers a cost-effective alternative to meeting today's highest technology demands. This layer combination of thin pure palladium covered by a flash of gold provides a coplanar surface that is both solderable and wire-bondable (gold and aluminum). The proposed technique significantly reduces the cost for capital investment (electroplating equipment) and consumable materials (precious metal) normally associated with the more traditional electrolytic nickel/electrolytic gold process.

## PROCESS DESCRIPTION

The proposed electroless nickel / electroless palladium / immersion gold (Ni/Pd/Au) plating process meets the technical requirements for BGA bonding, while offering the possibility for cost reduction. Table 1 and Figure 1 provide key process information. Following pre-treatment, an autocatalytic Nickel-Phosphorous layer (7-9 % P by wt.) is deposited. This deposit is then covered by a thin layer of autocatalytically plated pure palladium containing 99.99% Pd. Finally, a "flash" layer of immersion gold (30-50 nm) is deposited.

Process Step	Treatment Time (min)	Treatment Temp (°C)
Clean	3-6	35-45
Microetch	1 - 2	25-35
Acid Dip	>3	Ambient
Activate	1-3	20-25
<b>Electroless Nickel</b>	<b>15-25</b>	<b>80-90</b>
<b>Electroless Palladium</b>	<b>5-10</b>	<b>50-70</b>
<b>Immersion Gold</b>	<b>1-3</b>	<b>80-85</b>

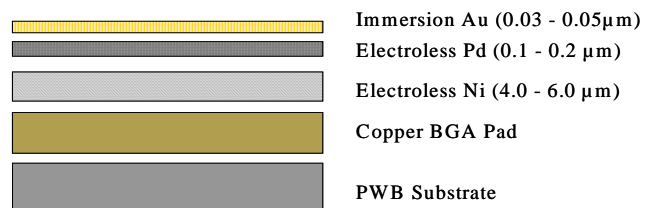


Fig 1. Illustration of layer build-up for Ni-Pd-Au process

## EXPERIMENTAL PROCEDURE

Experiments included both thermal cycling and extended heat aging. Two types of solder balls, eutectic tin-lead and SAC alloy (Sn, 3.5Ag, 0.6Cu), were soldered on mask-defined BGA pads on a commercially available FR4 substrate. Solder balls and surfaces were fluxed using Kester TSF6516. The major equipment used in the testing is as follows:

Test Equipment	Equipment Description
Solder Reflow Oven	SMT Model 200C
Thermal Cycling	Voetsch Model VT 7012 S2
High-Temperature Aging	ESPEC Model LHL-212
Ball Shear Testing	Dage Model 2400

### Sample Preparation - Thermal Cycling

For thermal cycle testing, 600- $\mu\text{m}$  diameter eutectic Sn-Pb solder balls were placed on 520- $\mu\text{m}$  solder mask-defined (SMD) pads. Following attachment of the solder balls, the selective finishes shown in Table 2 were subjected to 500 cycles from  $-55\text{ }^{\circ}\text{C}$  to  $+125\text{ }^{\circ}\text{C}$ , maintaining a 10-minute hold time at each temperature with a transfer time of three seconds.

Table 2 – Finishes for Thermal Cycle Tests All thicknesses reported in microns ( $\mu\text{m}$ )					
Finish Type	E'less Ni*	E'less Pd	Imm Au	E'less Au	Other
A	5.0	0.1	0.05	-	-
B	5.0	0.2	0.05	-	-
C	5.0	0.3	0.05	-	-
D	5.0	-	0.1	0.4	-
E	-	-	-	-	OSP

\* In all cases, 8.5 weight percent Phosphorus

Figure 2 shows the reflow profile for the eutectic (Sn/Pb) solder balls used for the thermal cycling investigations, denoting the peak temperature of  $215^{\circ}\text{C}$ .

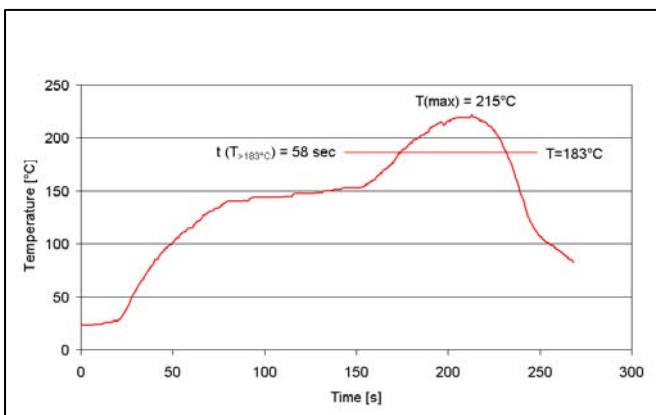


Fig. 2 Reflow profile for eutectic solder balls

### Sample Preparation - High-Temperature Aging

In the high-temperature aging test, 760- $\mu\text{m}$  SAC alloy solder balls were placed on 610- $\mu\text{m}$  SMD pads. Following ball attachment, the finishes shown in Table 3 were subjected to 1000 hours aging at  $150^{\circ}\text{C}$ .

Table 3 – Finishes for High-Temperature Aging Tests All thicknesses reported in microns ( $\mu\text{m}$ )					
Finish Type	E'less Ni	E'less Pd	Imm Au	E'lytic Ni	E'lytic Au
F	5.0	0.15	0.05	-	-
G				5.0	0.5

Figure 3 shows the reflow profile for the SAC alloy solder balls used for high-temperature aging investigations. As noted a peak temperature of  $242\text{ }^{\circ}\text{C}$  is achieved.

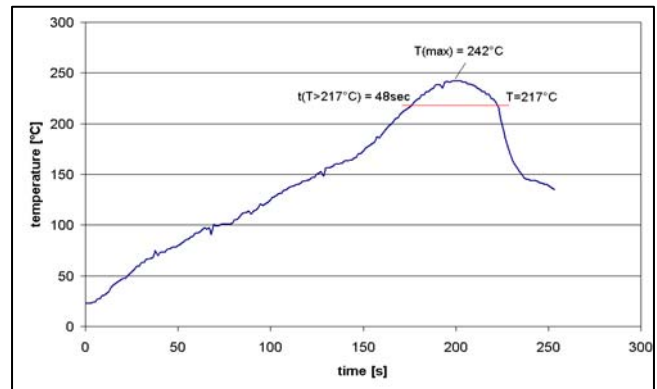


Fig. 3 Reflow profile for SAC alloy solder balls

Following high-temperature aging and thermal cycling, all specimens were subjected to ball-shear testing.

### Ball Shear Test

BGA-laminate manufacturers and assemblers will typically utilize ball shear tests. For test purposes, SMD pads were used to reduce the chance of “pad pullout”, thus more fully focusing on “ball-pad” fractures. Since the individual pads are solder mask defined (SMD), the mechanical resistance against a pad pullout is higher in comparison to a non-solder mask defined (NSMD) pad, which is typically found on the PWB side. Higher resistance against pad pullout will more readily cause the fracture to occur at the metallic layer, the IMC or within the solder, or any interface in between. Figure 4 illustrates the difference between solder balls mounted on SMD and NSMD pads.

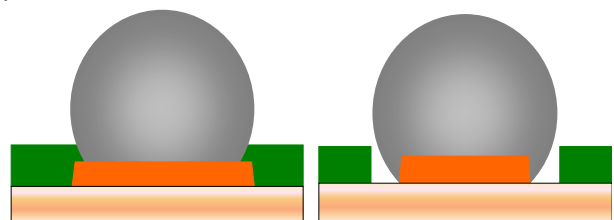
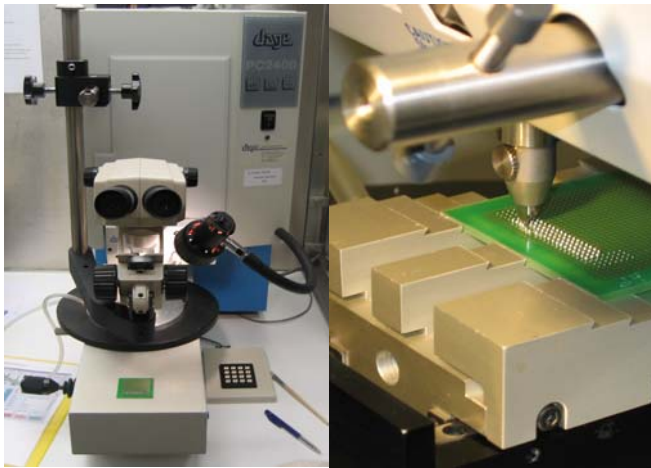
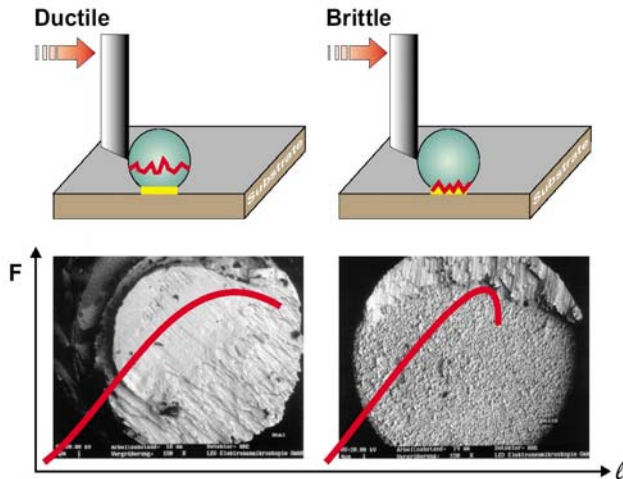


Fig. 4 Solder ball on SMD pad (left) and NSMD pad (right)



**Fig. 5** Dage Model 2400 (left) and detail of ball shear mechanism (right).

All ball shear tests were performed with a Dage Model 2400 device as shown in Figure 5. For each test segment, 30 balls were sheared and the resultant shear strain diagrams were plotted. As shown in Figure 6, fractures are classified as either “ductile” or “brittle” depending on the nature of the shear diagram. Diagrams with a steep descent after the maximum force is achieved represent the brittle interfacial fracture. Conversely, a gradual descent represents the desired ductile, plastic deformation that occurs within the solder or by pad pullout.



**Fig. 6** Comparison of ductile and brittle fracture modes for ball shear

In conducting the ball shear test, four distinct types of fracture are typically encountered and are illustrated in Figure 7. Modes 1 and 4 both represent ductile fracture. Mode 1 involves the lifting of the copper BGA pad from the PWB substrate and is known as “pad pullout”. Fracture mode 4 occurs within the solder ball itself. In both cases, the interfaces between the copper pads, plated finish and solder remain intact. Fracture modes 2 and 3 are indicative of brittle fracture. Mode 2 fractures will occur at the interface

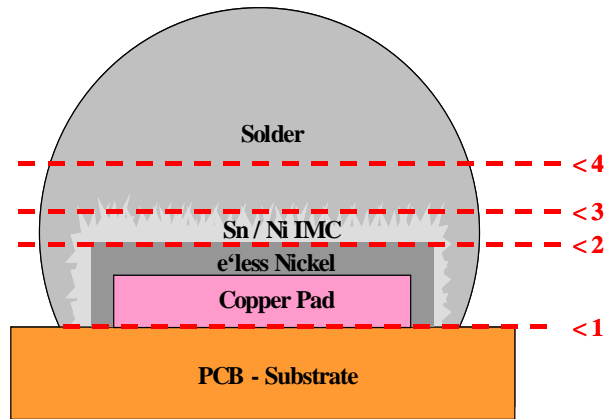


**Fig. 7** Location of fracture modes in relation to the solder ball and underlying substrates

between the plated nickel and the adjacent tin-nickel intermetallic compound (IMC). Likewise, mode 3 fractures will occur at the interface between the solder ball and the same IMC. Figures 8 through 10 show microscopic images of the fracture interfaces and typical shear diagrams.

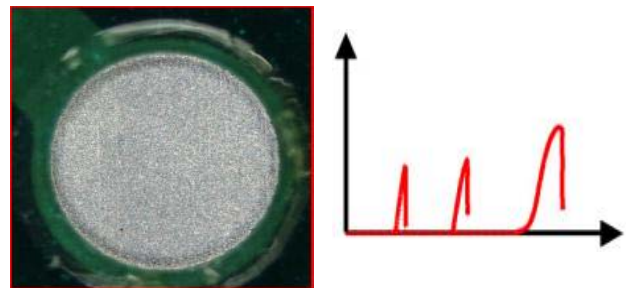


**Fig. 8** Fracture mode 2 interface showing 80-100 % exposed nickel surface and corresponding shear diagram.

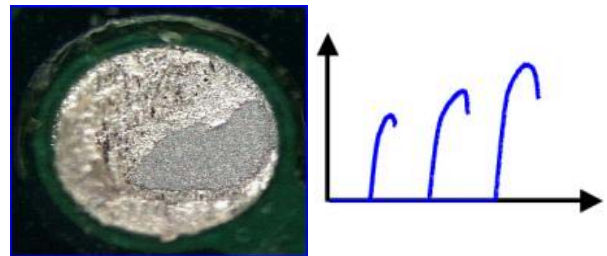


**Fig. 9** Fracture mode 3 interface showing 0-80% exposed nickel surface and corresponding shear diagram.

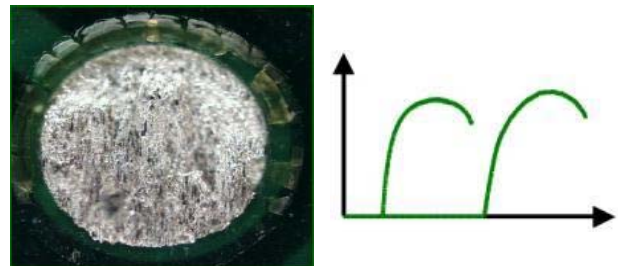


**Fig. 10** Fracture mode 4 interface showing no exposed nickel and corresponding shear diagram.

## Test Objectives

Although this part of the investigation is focused on performance with respect to BGA bonding, it is important to recall that the overall objective is for the selective finish to be wire-bondable as well as solderable. Currently, two alternative methods of providing a solderable and (gold) wire-bondable surface are (1) electroless nickel/electroless gold and (2) electrolytic nickel/electrolytic gold. Operating challenges have been realized for both approaches. Electroless gold is frequently troubled by extraneous plating or even plate-out in the worst cases. Electrolytic Ni/Au poses the problems of thickness distribution control and limitations for fine-pitch applications. Of course, both processes pose the common problem of high operating cost, since an electroless gold deposit of 0.3 to 0.5 micron is typically specified for wire bonding applications, while 0.5 to 1.0 micron of electrolytic gold can often be required.

## BALL SHEAR TEST RESULTS

As noted, ball shear tests were performed after samples were exposed to thermal cycling or high-temperature aging.

### Thermal Cycling Test Results (Eutectic Solder)

Ball shear tests were performed before and after 500 thermal cycles (-55 °C to +125 °C) using eutectic solder balls in all cases. The Ni-Pd-Au finish was evaluated with three different thicknesses of palladium: 0.1, 0.2 and 0.3 microns (Finish Types A, B and C). For comparison, an electroless nickel/electroless gold surface (Finish Type D) was also subjected to the same testing. Also, as a benchmark, an organic solderability preservative (OSP) was also tested. Since the use of an OSP creates a copper-tin IMC when soldered, it is less prone to brittle fracture in comparison to a nickel-tin IMC. As such, the ball shear tests performed on the OSP-treated surface should reflect the maximum obtainable values for the specified pad geometry and solder/alloy.

Figures 11 and 12 show the results of ball shear testing for the following Ni-Pd-Au deposit structure

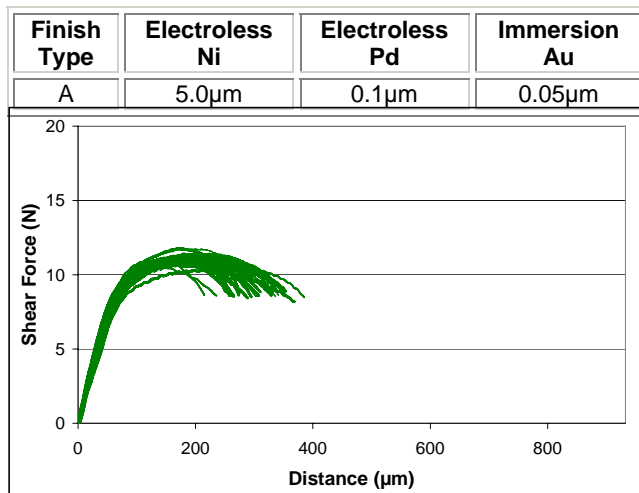


**Fig. 11** Ball shear diagram for Finish Type A, before thermal cycling

before and after thermal cycling. As the figures indicate, there is a slight reduction in the average maximum force required to shear the solder balls. However, the ductile nature of the fracture is maintained despite the exposure to thermal cycling.

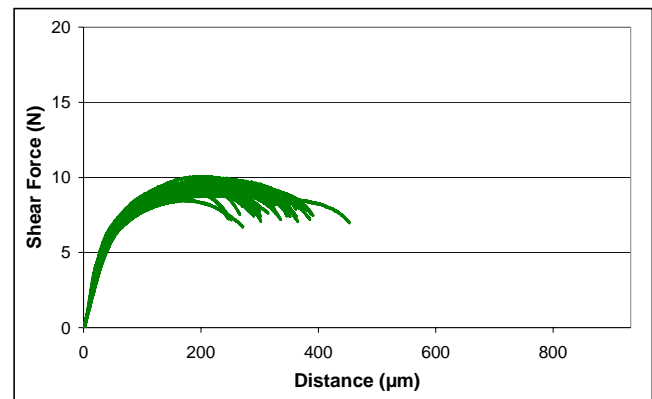


**Fig 12.** Ball shear diagram for Finish Type A, after thermal cycling

Figures 13 and 14 show the results of ball shear testing for the following Ni-Pd-Au deposit structure before and after thermal cycling.

Finish Type	Electroless Ni	Electroless Pd	Immersion Au
B	5.0µm	0.2µm	0.05µm

Again, the figures for the 0.2-micron palladium thickness show the same basic trend as that shown for

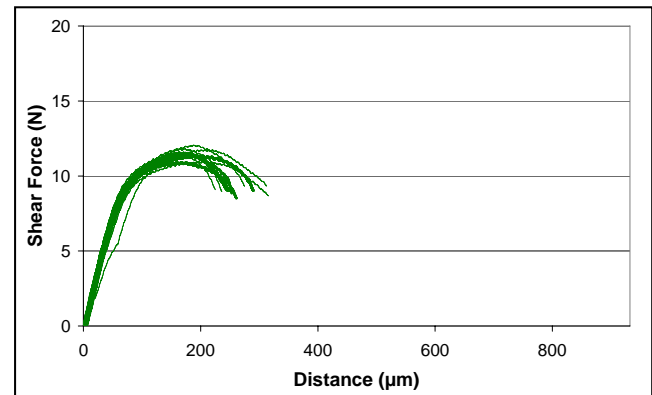


**Fig. 13** Ball shear diagram for Finish Type B, before thermal cycling

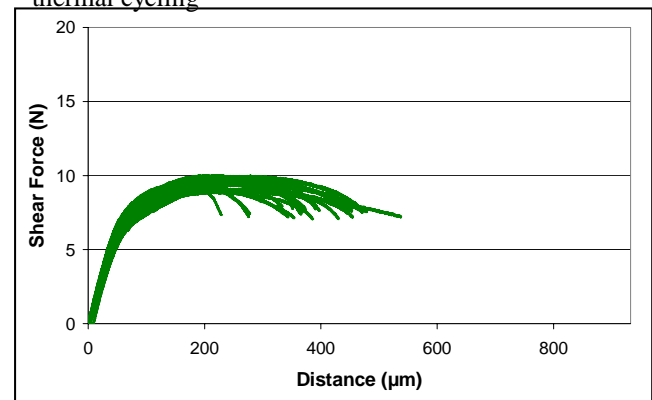


**Fig. 14** Ball shear diagram for Finish Type B, after thermal cycling

the 0.1-micron palladium thickness. Comparing the fracture behaviors, there is a clear effect of thermal cycling on the fracture modes. Even if the average maximum shear forces decrease after 500 thermal cycles, the plastic deformation of the solder joints/balls is seen to increase dramatically.

Figures 15 and 16 show the results of ball shear testing for the following Ni-Pd-Au deposit structure before and after thermal cycling.

Finish Type	Electroless Ni	Electroless Pd	Immersion Au
C	5.0 $\mu$ m	0.3 $\mu$ m	0.05 $\mu$ m

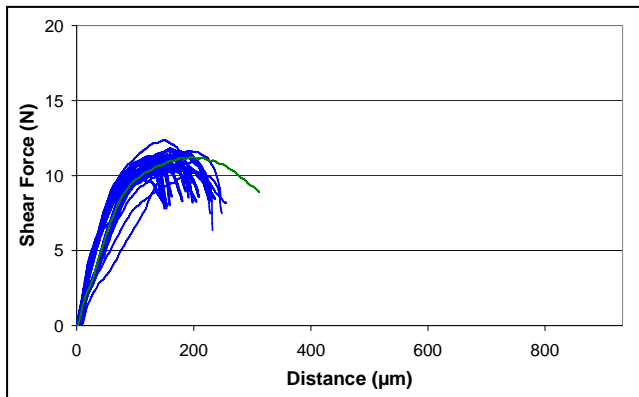


**Fig. 15** Ball shear diagram for Finish Type C, before thermal cycling

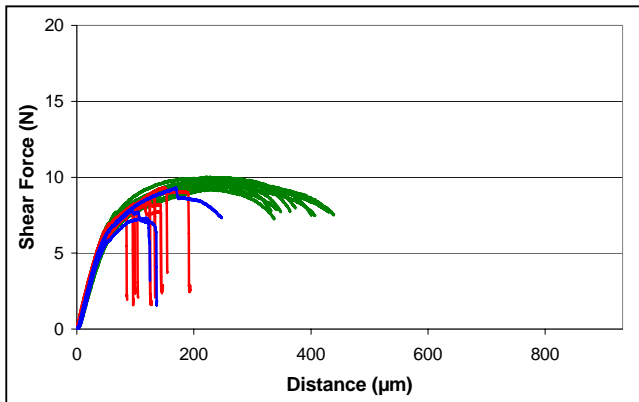


**Fig. 16** Ball shear diagram for Finish Type C, after thermal cycling

The shear diagrams shown in these two figures differ dramatically from the previous examples. Brittle fracture of the mode 3 type dominates the “as is” condition before thermal cycling (29 of 30 fractures). Although after thermal cycling the majority (18 of 30) of the fractures shift to the ductile mode, nearly one-third of the fractures are of the brittle mode 2 type with nearly 100 % exposed nickel surface after ball shear. For this test series, the weakest bond link was between the nickel layer and the nickel-tin IMC. Figures 15 and 16 clearly show that the palladium thickness has an impact on the failure mode.

Furthermore, the figures indicate that a palladium thickness of 0.3 microns makes the overall deposit significantly more reactive to thermal cycling than the previous thicknesses examined. By comparison, the 0.1- and 0.2-micron palladium deposits exhibited ductile fracture fully within the solder both before and after thermal cycling.

As noted previously, identical ball shear testing was also performed using an electroless nickel / electroless gold finish. In reality, the gold deposit consists of a very thin layer of immersion gold, followed by the electroless gold deposit. Figures 17 and 18 show the results of ball shear testing for the following electroless nickel / electroless gold structure before and after thermal cycling.

Finish Type	Electroless Ni	Immersion Au	Electroless Au
D	5.0 $\mu$ m	0.1 $\mu$ m	0.4 $\mu$ m

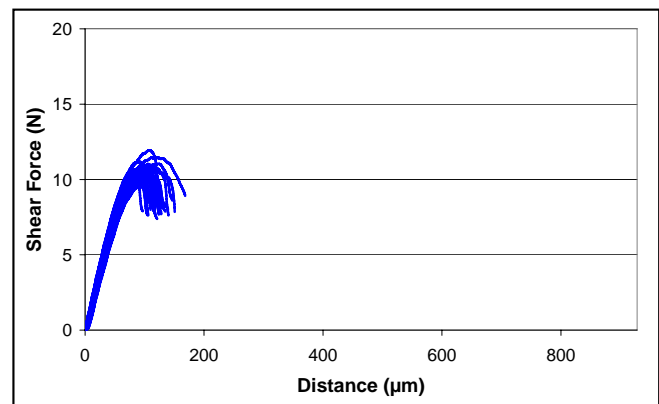


**Fig. 17** Ball shear diagram for Finish Type D, before thermal cycling

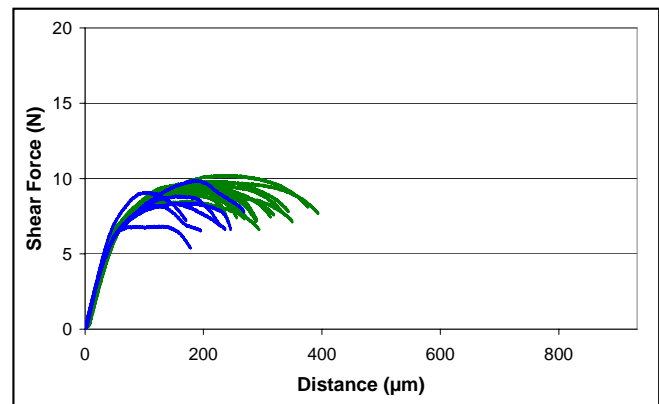


**Fig. 18** Ball shear diagram for Finish Type D, after thermal cycling

Figure 17 shows that ball shear testing of the electroless nickel / electroless gold finish also yielded only brittle fractures in the “as received” condition (before thermal cycling), similar to the Ni-Pd-Au deposit with 0.3-micron palladium. Likewise, Figure 18

shows that shearing after thermal cycling resulted in a more ductile response, although many Type 3 brittle fractures still occurred.

As previously mentioned, testing of the OSP-treated surface was performed to simulate the best results for the Ni-Pd-Au deposit that could be expected. Figures 19 and 20 show the results of ball shear testing for the OSP-treated copper surface (Finish Type E) before and

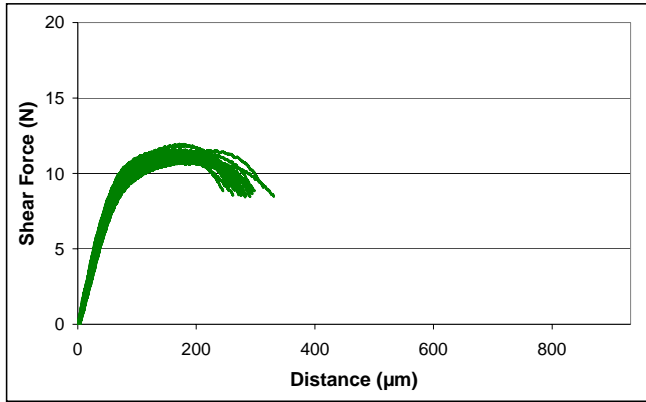


**Fig. 19** Ball shear diagram for Finish Type E (OSP), before thermal cycling

and after thermal cycling. Comparing the results shown in Figures 11 and 13 with those of Figure 19 indicate that the Ni-Pd-Au deposits with 0.1- and 0.2-microns of palladium performed almost identically to the OSP-treated surface prior to any thermal cycling. In fact, the thinner palladium deposit actually exhibited a slightly more ductile behavior than the OSP-treated sample. Similarly, after 500 thermal cycles, the Ni-Pd-Au deposits with 0.1- and 0.2-microns of palladium virtually matched the performance of the OSP-treated samples. In this case, the Ni-Pd-Au deposit with 0.2-microns of palladium is shown to give a slightly more ductile response.

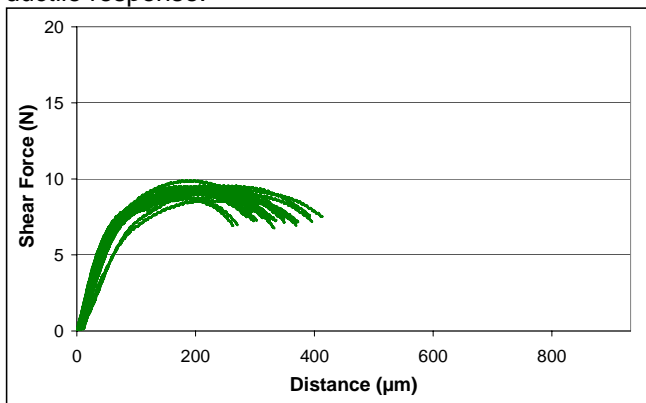


**Fig. 20** Ball shear diagram for Finish Type E (OSP), after thermal cycling

### High-Temperature Aging Test Results (SAC-Alloy)

Ball shear tests were also performed before and after high-temperature aging (1000 hours at 150°C). In this case, solder balls of SAC-alloy were used for all testing. The Ni-Pd-Au finish was evaluated with a palladium thickness of 0.15 micron (Finish Type F). In this test series, an electrolytic nickel / electrolytic gold surface was subjected to the same testing for comparison.

Figures 21 and 22 show the results of ball shear testing for the following Ni-Pd-Au deposit structure before and after high-temperature aging.

Finish Type	Electroless Ni	Electroless Pd	Immersion Au
F	5.0µm	0.15µm	0.05µm

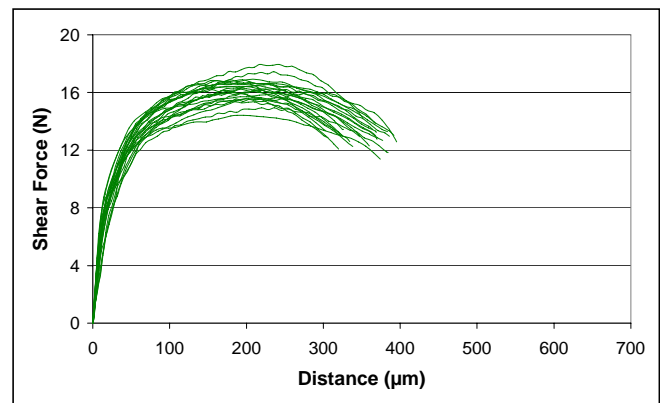


**Fig. 21** Ball shear diagram for Finish Type F, before high-temperature aging

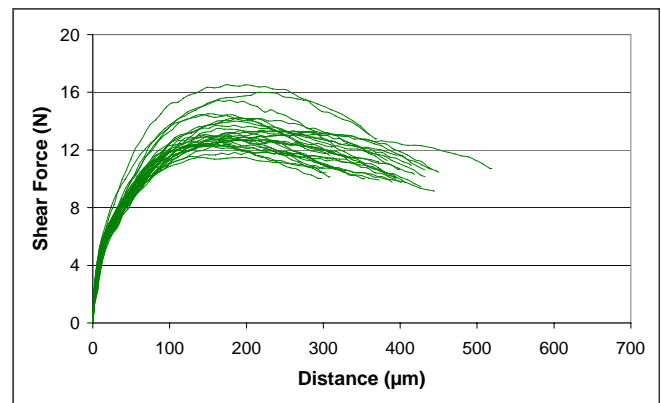


**Fig. 22** Ball shear diagram for Finish Type F, after high-temperature aging

Again, the same behavior shown previously in the thermal cycling tests is exhibited. Generally, prior to any heat treatment, the maximum required shear force is somewhat higher, but a more ductile fracture mode is exhibited after the high-temperature aging.

Because the pad dimensions differed between the testing of eutectic solder and SAC-alloy, the actual

shear force values cannot be directly compared. Only the shape of the shear diagrams and fracture modes can be accurately compared. As such, in comparing the shape and length (i.e. deformation distance) of the diagrams for eutectic solder on the Ni-Pd-Au surface with 0.1- $\mu\text{m}$  and 0.2- $\mu\text{m}$  of palladium (Fig 11 and 13, respectively) to those of Figure 21, it is clear that prior to any thermal exposure the SAC-alloy is at least equivalent to that of the eutectic solder in terms of joint strength. Prior to any heat aging, ball shear testing of the Ni-Pd-Au finish demonstrated ductile fracture with plastic deformation of the SAC-alloy ball in each case. Following high-temperature aging, only ductile fractures were reported and in some cases the deformation exceeded 400 microns, or more than 60-percent of the pad diameter.

Figures 23 and 24 show the results of ball shear testing for the following electrolytic nickel / electrolytic gold deposit before and after high-temperature aging.

Finish Type	Electrolytic Ni	Electrolytic Au
G	5.0 $\mu\text{m}$	0.5 $\mu\text{m}$

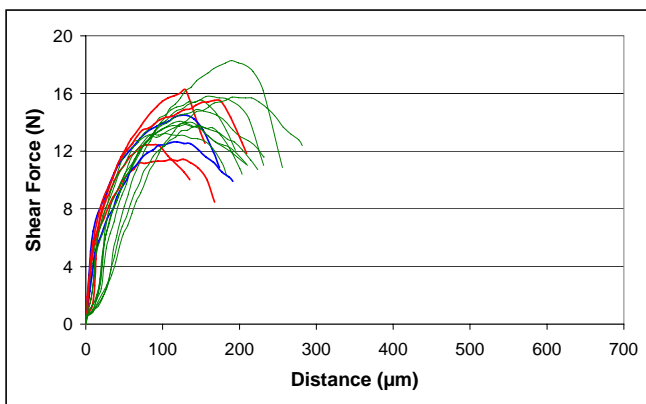


**Fig. 23** Ball shear diagram for Finish Type G, before high-temperature aging

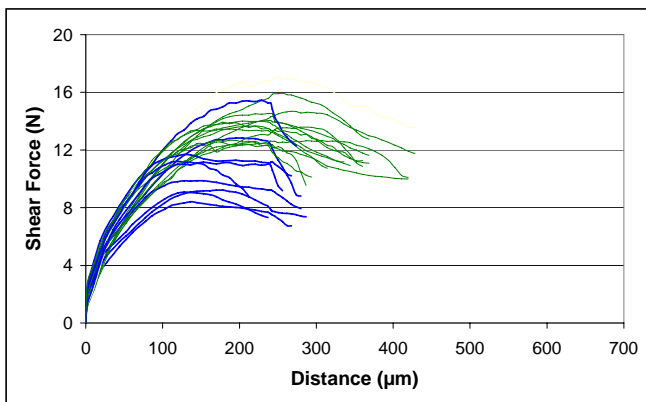


**Fig. 24** Ball shear diagram for Finish Type G, after high-temperature aging

In Figure 24, it is evident that the bond created by soldering the SAC-alloy to a conventional electrolytic nickel / electrolytic gold finish exhibited several instances of Mode 2 and Mode 3 brittle fracture. In addition, the deformation during the ductile fractures averaged approximately 40-percent less than that achieved with the Ni-Pd-Au finish. After high-temperature aging, nearly one-third of the tests still resulted in Mode 3 brittle fracture, although heat aging did improve the nature of the ductile fractures, resulting in a more plastic deformation.

## CONCLUSIONS / DISCUSSION

As shown herein, the Ni-Pd-Au process is a technically viable alternative to either the electroless nickel/electroless gold or electrolytic nickel/electrolytic gold processes, currently used for multi-purpose bonding where both soldering and wire bonding are required. Based on these investigations, the following conclusions are offered:

1. Based on the results of ball shear testing, with an optimized palladium thickness the Ni-Pd-Au finish exhibited superior performance in comparison to both electroless nickel/electroless gold and electrolytic nickel/ electrolytic gold using eutectic solder and SAC-alloy balls, respectively.
2. The thickness of the palladium layer in the Ni-Pd-Au deposit has a significant effect on the fracture mode of bonded BGAs. Based on these ball shear investigations, optimum results are achieved with less than 0.2 microns of palladium. Tests conducted before and after thermal cycling as well as high-temperature aging confirm that the optimum performance occurs with deposits having palladium layers within this thickness range. Applying a thicker deposit leads to brittle fracture, as proven with a palladium thickness of only 0.3 microns.
3. In all ball shear tests, both thermal cycling and high-temperature aging improve the ductility of the bonds to the various finishes examined. Although the maximum sustainable shear force is always reduced following such thermal conditioning, the incidence of brittle fracture (Mode 2 or 3) is consistently shifted to a more ductile fracture of a more plastic deformation.
4. Based on ball shear test results for an OSP-treated surface, soldering to the Ni-Pd-Au deposit creates a bond with shear characteristics that are more similar to that achieved with the copper-tin IMC (created by ball-attach to the OSP-treated copper surface) than to the shear characteristic of a conventional nickel-tin IMC (created by bonding eutectic solder or SAC-alloy to either electroless nickel/gold or electrolytic nickel/gold finishes). The

similarities in fracture mode and deformations are apparent both before and after thermal cycling.

5. The results of ball shear tests performed with eutectic solder balls on a conventional electroless nickel/electroless gold finish show an extremely high incidence of brittle fracture in the "as received" condition (before thermal cycling). After 500 thermal cycles, some brittle fracture still occurred, but the overall response of the bonds to the shear test was more ductile in nature.
6. The results of ball shear tests performed with SAC-alloy solder balls on a conventional electrolytic nickel/electrolytic gold finish show a moderate-to-high incidence of brittle fracture both before and after thermal cycling. Some brittle fracture still occurred following 1000 hours of heat treatment, but overall, the bonds exhibited the same tendency toward a more ductile response.

The ball shear results described in this evaluation confirm the applicability of the Ni-Pd-Au finish for BGA bonding. Because the process involves only chemical deposition, additional improvements in terms of better planarity and conformity to pad geometry can be achieved in comparison to electrolytic plating techniques. In addition, as shown in Figure 25, use of the Ni-Pd-Au finish offers the potential for fabrication cost reductions by eliminating much of the precious metal expense.

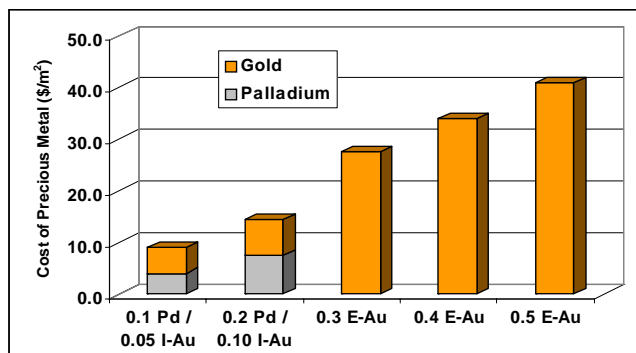


**Fig. 25** Relative precious metal cost of Ni-Pd-Au process vs. Electroless or Electrolytic Gold

The results of these investigations also indicate that the Ni-Pd-Au process provides improved bonding results for soldering BGAs of SAC-alloy composition. As lead-free initiatives become adopted globally within the electronics industry, the use of eutectic solder will become less common while solder compositions such as the SAC-alloy will become more prevalent.

The suitability of the Ni-Pd-Au process for gold and aluminum wire bonding was previously detailed in the paper titled, "Electroless Nickel / Electroless Palladium / Immersion Gold Process for Gold- and Aluminum-Wire Bonding Designed for High-Temperature Applications", presented at the 2004 Pan Pacific

Microelectronics Symposium, sponsored by SMTA. In that part of the evaluation, the Ni-Pd-Au deposit was shown to be a viable finish for both gold- and aluminum-wire bonding. Although that particular evaluation focused on ceramic substrate applications, the results are applicable for conventional FR4 substrates as used in this examination. The combined results of these investigations clearly indicate that the Ni-Pd-Au process, commercially known as SolderBond™, offers a cost-effective solution for multi-purpose assembly requiring a surface that is both solderable and wire-bondable.

## References

1. Dr. Halser, Bohn, Dr. Krause, Dr Nowotnick, Pape, Schulz, "Shear Test of BGA-Solder Balls", Fraunhofer-Institut für Zuverlässigkeit und Mikrointegration (IZM) Abteilung Baugruppenttechnologie und Verbindungstechniken; Atotech, Berlin; March 1998
2. Dr.Ing. M. Schneider-Ramelow, Dr.Ing. K.D. Lang, Fraunhofer-Institut für Zuverlässigkeit und Mikrointegration IZM-Berlin; Dr.Ing F. Rudolf, Dr.Ing. I. Witte, TU Dresden Fakultät Elektrotechnik und Informationstechnik, Institut für Halbleiter- und Mikrosystemtechnik und Institut für Feinwerktechnik; Dr.Ing. D. Metzger, Atotech, "Chip on Board (COB) – Technik in hermetisch gekapselten Mikrosystemen für den Einsatz im rauen und feuchten Umfeld der Meeresbiologie"; Atotech, Berlin; March 2003
3. „Investigations on Brittle Fracture of BGA Assemblies on Electroless Nickel / Immersion Gold Surface Finishes“, Atotech Berlin, Atotech Rock Hill, May 1999
4. „Methode of Measuring the Phosphorous Content“, Atotech, Berlin, December 2001
5. "Impact of ENIG Thickness to Solder Joint Integrity on BGA Pads", Atotech, Berlin, May 2004
6. Dr. Schreier, Burkhart, "High Performance Coplanar Finishes for BGAs and High Density Substrates", Atotech, Berlin, November 2000